20000727238

SECURITY CLASSIFICATION OF THIS PAGE (When Data Entered)

REPORT DOCUMENTATION PAGE

READ INSTRUCTIONS BEFORE COMPLETING FORM

1. REPORT NUMBER: Report No. 3EX
2. GOVT ACCESSION NO.
3. RECIPIENT'S CATALOG NUMBER

4. TITLE (and Subtitle): Measurement of Polarized Light Scattering Via the Mueller Matrix
5. TYPE OF REPORT & PERIOD COVERED: Technical Report, #3
6. PERFORMING ORG. REPORT NUMBER

7. AUTHOR(s): Randall C. Thompson, Jerold R. Rottiger and Edward S. Fry
8. CONTRACT OR GRANT NUMBER(s): N00014-75-C-0537

9. PERFORMING ORGANIZATION NAME AND ADDRESS
Department of Oceanography
Texas A&M University
College Station, Texas 77843

10. PROGRAM ELEMENT, PROJECT, TASK AREA & WORK UNIT NUMBERS

11. CONTROLLING OFFICE NAME AND ADDRESS
Office of Naval Research
Code 480
Arlington, Virginia 22217

12. REPORT DATE: 8 September 1979
13. NUMBER OF PAGES: 45p.

14. MONITORING AGENCY NAME & ADDRESS (if different from Controlling Office)
Texas A&M Research Foundation
Faculty Exchange H
College Station, Texas 77843

15. SECURITY CLASS. (of this report): Unclassified
15a. DECLASSIFICATION/DOWNGRADING SCHEDULE

16. DISTRIBUTION STATEMENT (of this Report)

Approved for public release, distribution unlimited

17. DISTRIBUTION STATEMENT (of the abstract entered in Block 20, if different from Report)

18. SUPPLEMENTARY NOTES

DDC RECEIVED SEP 28 1979 A

19. KEY WORDS (Continue on reverse side if necessary and identify by block number)

Light Polarization, Measurements Mueller

20. ABSTRACT (Continue on reverse side if necessary and identify by block number)

A new instrument for rapid and accurate measurement of the Mueller matrix is described. Distinct measurements of all sixteen elements are made simultaneously and with an absolute accuracy of 1% to 5%. The instrument employs electro-optic modulators. Results are presented for several simple optical devices and systems.

DD FORM 1 JAN 73 1473 EDITION OF 1 NOV 65 IS OBSOLETE
S/N 0102-014-6601

SECURITY CLASSIFICATION OF THIS PAGE (When Data Entered)

AD A074431

DDC FILE COPY

MEASUREMENT OF POLARIZED LIGHT SCATTERING VIA THE MUELLER MATRIX

by

Randall C. Thompson, Jerold R. Bottiger, and Edward S. Fry

Report No. 3~~BX~~

The research described in this report was
funded by
The Ocean Science and Technology Division
of the
Office of Naval Research

Contract N00014-75-C-0537

Department of Physics
Texas A&M University
College Station, Texas 77843

4 September, 1979

The material in this report has been submitted for publication to Applied Optics.

MEASUREMENT OF POLARIZED LIGHT INTERACTIONS VIA THE MUELLER MATRIX

Randall C. Thompson, Jerold R. Bottiger, and Edward S. Fry

Texas A&M University

Department of Physics

College Station, Texas 77843

ABSTRACT

A new instrument for rapid and accurate measurement of the Mueller matrix is described. Distinct measurements of all sixteen elements are made simultaneously and with an absolute accuracy of 1% to 5%. The instrument employs electro-optic modulators. Results are presented for several simple optical devices and systems.

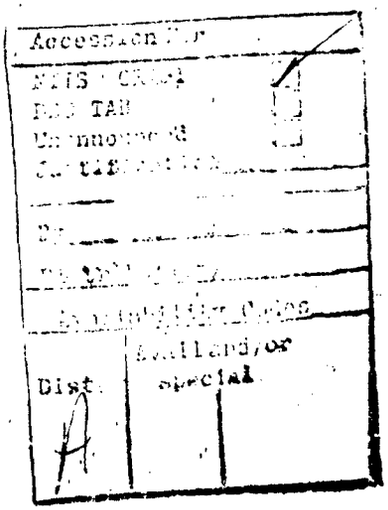

I. INTRODUCTION

When light in some arbitrary polarization state is incident on a medium, the polarization state of the scattered, transmitted, or reflected light can be related to the polarization state of the incident light by a 4x4 matrix.[1-3] This matrix, frequently called the Mueller matrix, is a characteristic of the medium. It depends on wavelength, and, in the case of light scattering, is a function of scattering angle. It is a necessary and major part of the complete optical description of a medium.

The matrix provides essential input information into calculations of the light field in planetary atmospheres and in the oceans.[4-7] It thus has applications in the fields of climatology, illumination, communications, and visibility. Further the matrix itself gives valuable information about the biological and physical properties of the scattering particulates. This line of inquiry has been used in recent studies of ocean hydrosols.[8-10]

Calculations of the matrix for scattering of electromagnetic radiation are in the early stages of development. In general, only simple geometries have been considered: (1) the homogeneous sphere with arbitrary size;[2,11] (2) infinite circular cylinders;[12,13] and (3) spheroidal particles.[14] Recent developments are, however, showing considerable promise for calculations involving arbitrarily shaped,

inhomogeneous particles.[15-17]

Few efforts have been made to measure the entire matrix due to the difficulties associated with using conventional techniques. These involve making intensity measurements with various independent combinations of polarizers and retarders in the incoming and outgoing light beams. The sixteen matrix elements are obtained from the frequently small differences between these relatively large measured quantities. Such measurements were pioneered by Pritchard and Elliott[18] and by Rozenberg;[19-20] they were studying the optical properties of the atmosphere. Perhaps the best example of the conventional method of matrix measurements is the work of Holland and Gagne[21]; their principle objective was to find the correlations between matrix elements of randomly oriented irregular particles and those due to the spherical particles having the "same" size distribution and refractive index. Other conventional measurements directed toward oceanic hydrosols and toward obtaining complete optical properties of ocean waters have been made by Beardsley[22] and by Kadyshevich, et. al.[8-10]

Optical polarization modulators can significantly enhance the accuracy of polarization measurements. This concept was first used in measurements of the Stokes vector of a beam of light.[23] It was quite successful and has been used for circular dichroism measurements[24] and for polarimetry in astronomy.[25-26] Many variants have appeared in the recent literature.[27-30]

Mueller matrix measurements using polarization modulation techniques were first made by Hunt and Huffman[31] and then by Thompson and Fry.[32] The former used a single photoelastic type modulator; thus they could in general only measure combinations of matrix elements. Nevertheless, their results provided a major advance in the speed and accuracy with which matrix measurements could be made.[33] Instruments using a single modulator have seen recent use in biophysical applications.[34] An instrument using two polarization modulators has been recently proposed and analyzed by Azzam.[35]

In this paper we will describe the four modulator photopolarimeter developed by Thompson et. al.[32,36-37] It provided the first direct and simultaneous measurement of all sixteen elements of the Mueller matrix. In light scattering applications it requires approximately two minutes for measurement of the entire matrix over scattering angles from 5^0 to 170^0 with an accuracy of better than 3%. This compares with ~2 hours for measurements with ~10% accuracy using a conventional method.[9] This ability to make complete measurements very rapidly is of extreme importance when one is studying samples that are changing in time, for example, ocean water and biologically active suspensions in general.

Since light scattering has been our main interest, this paper will be presented from that point of view. The concepts, nevertheless, apply equally well to transmission and reflection studies.

II. THEORETICAL BACKGROUND

To mathematically describe the polarization state of a general beam of light, we will use the Stokes vector representation,[2-3]

$$\vec{S} = \begin{vmatrix} I \\ Q \\ U \\ V \end{vmatrix} \quad . \tag{1}$$

The linear interaction of an optical device with a beam of light can be described as a transformation of an incident Stokes vector $\vec{S}_i$ into an emerging Stokes vector $\vec{S}_e$,

$$\vec{S}_e = \underline{A}\, \vec{S}_i \quad . \tag{2}$$

Here A is the 4x4 matrix known as the Mueller (or phase) matrix. It is a characteristic of the optical device or system. Matrices representing linear retarders and polarizers are easily derived.[3] The transformation of an initial Stokes vector by a sequence of optical devices is given by the matrix which is the sequential product of the matrices representing each device,

$$\underline{A} = \underline{A}_n \times \ldots\ldots \underline{A}_3 \times \underline{A}_2 \times \underline{A}_1 \quad . \tag{3}$$

The Mueller matrix representing a scattering system is given by $\underline{F}(\theta)$, where θ is the scattering angle (See Fig. 1). For convenience in the present discussion we are suppressing the azimuthal dependence; this is not a fundamental restriction. For a system of randomly oriented and isotropically distributed particles, $\underline{F}$ in fact has no azimuthal dependence.

The elements of $\underline{F}$ are denoted by $f_{ij}(i,j=1,2,3,4)$. It is particularly instructive to work with the reduced matrix

$$\underline{F}'(\theta) = \frac{\underline{F}(\theta)}{f_{11}(\theta)} \tag{4}$$

In the reduced matrix all elements are restricted by

$$-1 \leq f'_{ij}(\theta) \leq +1 , \tag{5}$$

and, of course, $f'_{11}(\theta)$ is identically plus one. We will measure $\underline{F}'(\theta)$ directly.

For typical scattering systems the sixteen elements of $\underline{F}(\theta)$ are generally not all independent. Symmetries within the population of scattering particles and within individual particles serve to reduce the number of independent elements. Van de Hulst[2] and Perrin[1] have discussed such symmetries in detail. By measuring the entire scattering matrix the symmetries within it can be determined and these

can then be related to the symmetries in the scattering system. Kadyshevich et. al. have found some symmetries in oceanic hydrosols by using this approach.[8-10]

III. PHOTOPOLARIMETER THEORY

In this section we will present the theory behind the operation of our four modulator photopolarimeter. There are, of course, many variants of our instrument that can be used to obtain distinct, simultaneous measurement of all elements of the Mueller matrix. The calculational procedures are essentially the same for all of them. Therefore, for simplicity, we will restrict the discussion to our specific instrument.

A schematic diagram of our optical system is shown in Fig. 1. We will take the reference plane for our measurements to be horizontal. This is identical to the scattering plane. MOD1,2,3, and 4 are the polarization modulators. They are electro-optic modulators whose optical retardance is voltage variable. The angle between the principle axis of each modulator and the reference plane is denoted by $\gamma_i (i=1,2,3,4)$. POL1 and POL2 are linear polarizers with transmission axes parallel to the reference plane. The sample whose matrix is to be measured is denoted by $\underline{F}$.

We now require the Mueller matrix for each of the optical elements.[3] For POL1 and POL2 in the required orientation, the matrix is

$$\underline{P}_j = \frac{1}{2} \begin{vmatrix} 1 & 1 & 0 & 0 \\ 1 & 1 & 0 & 0 \\ 0 & 0 & 0 & 0 \\ 0 & 0 & 0 & 0 \end{vmatrix} \qquad (6)$$

The matrix for MOD1 and MOD4 with $\gamma_{1(4)} = \pi/4$ is

$$\underline{M}_{1(4)} = \begin{vmatrix} 1 & 0 & 0 & 0 \\ 0 & \cos\delta_{1(4)} & 0 & \sin\delta_{1(4)} \\ 0 & 0 & 1 & 0 \\ 0 & -\sin\delta_{1(4)} & 0 & \cos\delta_{1(4)} \end{vmatrix} . \qquad (7)$$

For MOD2 and MOD3 with $\gamma_{2(3)} = 0$ it is

$$\underline{M}_{2(3)} = \begin{vmatrix} 1 & 0 & 0 & 0 \\ 0 & 1 & 0 & 0 \\ 0 & 0 & \cos\delta_{2(3)} & -\sin\delta_{2(3)} \\ 0 & 0 & \sin\delta_{2(3)} & \cos\delta_{2(3)} \end{vmatrix} . \qquad (8)$$

In the above matrices δ_i (i=1,2,3,4) is the retardance of the ith modulator. The matrix to be measured is given by

$$\underline{F} = \begin{vmatrix} f_{11} & f_{12} & f_{13} & f_{14} \\ f_{21} & f_{22} & f_{23} & f_{24} \\ f_{31} & f_{32} & f_{33} & f_{34} \\ f_{41} & f_{42} & f_{43} & f_{44} \end{vmatrix} . \qquad (9)$$

POL1 insures that the initial state of polarization is given by

$$S_o = I_o \begin{vmatrix} 1 \\ 1 \\ 0 \\ 0 \end{vmatrix} \quad , \tag{10}$$

where the explicit dependence on intensity has been factored out as I_o. POL 2 ensures that the light incident on the PMT has the Stokes vector

$$S_f = I_f \begin{vmatrix} 1 \\ 1 \\ 0 \\ 0 \end{vmatrix} \quad , \tag{11}$$

where again the explicit dependence on the intensity has been factored out. It is clear from Eq. (11) that the polarization of the light incident on the PMT is constant. Thus polarization dependences in the PMT cannot lead to systematic errors. This has frequently not been the case in previous polarization studies.

From Eq. (11) we see that we need only compute the intensity I_f which results when S_o is operated on by the optical system. Using the Stokes-Mueller calculus we have

$$S_f = I_o \, (P_2 M_4 M_3 F M_2 M_1) S_0 \quad . \tag{12}$$

Using Eqs. 6-10 and performing the multiplications indicated in Eq. (12), we find

$$
\begin{aligned}
I_f = \frac{I_o}{2} (&f_{11} \\
&+f_{12} \cos \delta_1 \\
&+f_{13} \sin \delta_1 \sin \delta_2 \\
&-f_{14} \sin \delta_1 \cos \delta_2 \\
&+f_{21} \cos \delta_4 \\
&+f_{22} \cos \delta_1 \cos \delta_4 \\
&+f_{23} \sin \delta_1 \sin \delta_2 \cos \delta_4 \\
&-f_{24} \sin \delta_1 \cos \delta_2 \cos \delta_4 \\
&+f_{31} \sin \delta_3 \sin \delta_4 \\
&+f_{32} \cos \delta_1 \sin \delta_3 \sin \delta_4 \\
&+f_{33} \sin \delta_1 \sin \delta_2 \sin \delta_3 \sin \delta_4 \\
&-f_{34} \sin \delta_1 \cos \delta_2 \sin \delta_3 \sin \delta_4 \\
&+f_{41} \cos \delta_3 \sin \delta_4 \\
&+f_{42} \cos \delta_1 \cos \delta_3 \sin \delta_4 \\
&+f_{43} \sin \delta_1 \sin \delta_2 \cos \delta_3 \sin \delta_4 \\
&-f_{44} \sin \delta_1 \cos \delta_2 \cos \delta_3 \sin \delta_4).
\end{aligned}
\tag{13}
$$

All elements of $\underline{F}$ appear in this result, and each is multiplied by a unique combination of trigonometric functions.

The modulator retardances are varied sinusoidally at different frequencies ω_i,

$$\delta_i = \delta_{oi} \cos \omega_i t. \tag{14}$$

Here δ_{0i} is the amplitude of the retardance of the ith modulator. With this form for the retardance the functions sin δ_i and cos δ_i can be expanded in terms of Bessel functions of the retardation amplitudes,

$$\cos \delta_i = J_0(\delta_{0i}) - 2J_2(\delta_{0i}) \cos 2\omega_i t + 2J_4(\delta_{0i}) \cos 4\omega_i t - \ldots \quad (15)$$

$$\sin \delta_i = 2J_1(\delta_{0i}) \cos \omega_i t - 2J_3(\delta_{0i}) \cos 3\omega_i t + \ldots \quad (16)$$

These results are substituted into Eq. (13) and all products are expanded to give the Fourier components. We find that the intensity, I_f, has a DC component plus sinusoidal terms with amplitudes proportional to products of the Bessel functions and the matrix elements f_{ij}. The frequency of every Fourier component is given by

$$k\omega_1 \pm l\omega_2 \pm m\omega_3 \pm n\omega_4, \qquad k,l,m,n = 0,1,2,3,\ldots. \quad (17)$$

For example we give the expansion of the coefficient of f_{14} in equation (13),

$$\begin{aligned}\sin \delta_1 \cos \delta_2 = {} & 2 J_1(\delta_{01}) J_0(\delta_{02}) \cos \omega_1 t - 2 J_3(\delta_{01}) J_0(\delta_{02}) \cos 3\omega_1 t \\ & -2 J_1(\delta_{01}) J_2(\delta_{02}) \{\cos(\omega_1 + 2\omega_2)t + \cos(\omega_1 - 2\omega_2)t\} \\ & +2 J_3(\delta_{01}) J_2(\delta_{02}) \{\cos(3\omega_1 + 2\omega_2)t + \cos(3\omega_1 - 2\omega_2)t\} \\ & + \ldots.\end{aligned} \quad (18)$$

Thus the frequencies at which f_{14} appears in the intensity are given by Eq. (17) with m=n=0, k=odd integers, and l=even integers and

zero. The linear combinations of primary frequencies at which each matrix element appears as a leading term in the Fourier expansion of the intens'ty are given in Fig. 2.

To insure the distinct measurement of each matrix element, we will require that there be a unique reference frequency in the Fourier spectrum of Eq. (13) corresponding to each matrix element. Experimental considerations make it desirable that the selected component be one of the leading terms in the Fourier expansion and that the frequency be compatible with standard phase sensitive detection techniques (<100 kHz). We are free to adjust the four primary frequencies, ω_i, and the amplitude of the retardances, δ_{0i}, sc as to satisfy these requirements.

We set the amplitudes of the retardances so as to make

$$J_0 (\delta_{0i}) = 0, \tag{19}$$

or

$$\delta_{0i} = 2.404 \text{ radians}. \tag{20}$$

The DC term is thereby removed from the expansion of cos δ_i in Eq. (15). The most important consequence of this is that the DC component of I_f is proportional only to f_{11}.

In selecting the four modulator frequencies, ω_i, we note that

if they all have rational ratios then the requirement of a unique reference frequency for each matrix element is impossible unless we can truncate the expansions of cos δ_i and sin δ_i. Such a truncation is reasonable since $J_n(\delta_{0i})$ rapidly approaches zero with increasing n. Further, the four primary frequencies must be chosen so that the frequencies in the Fourier expansion of I_f are not so close as to require unreasonably long time constants in the detection system to distinguish them.

The set of primary frequencies we have chosen for the present instrument is

$$\begin{aligned} \nu_1 &= 41.0 \text{ kHz} \\ \nu_2 &= 0.3 \text{ kHz} \\ \nu_3 &= 1.0 \text{ kHz} \\ \nu_4 &= 10.0 \text{ kHz} \end{aligned} \tag{21}$$

The resulting reference frequencies which we have selected for the sixteen matrix elements are given in Figure 2. Each of these reference frequencies is indeed unique if the expansions given in Eqs. (15) and (16) are truncated at J_6 and J_5 respectively. Extending each expansion one more term, some degeneracies result; the largest of these at our selected signal frequencies is

$$\frac{\text{coeff } f_{32}}{\text{coeff } f_{31}} = \frac{2\, J_2(\delta_{01})\, J_3(\delta_{03})\, J_7(\delta_{04})}{2\, J_1(\delta_{03})\, J_1(\delta_{04})} = 1.9 \times 10^{-4} \,, \tag{22}$$

at the frequency of 9.0 kHz. This is well within our experimental error and is thus acceptable. Finally, with this choice of primary frequencies, Eqs. (21), all frequencies in Fourier spectrum of I_f are separated by at least 100 Hz. Thus they are easily distinguished with lock-in detectors and short time constants.

IV. EXPERIMENTAL APPARATUS

A. Optical System

The light source is a laser (See Fig. 1). We have used both a He-Ne laser (5mw. at 633 nm) and a He-Cd laser (20 mw at 442 nm). POL 1 and POL 2 are Glan prism polarizers which provide an extinction ratio of 5×10^{-5}. MOD1 and MOD2 are the retardance modulators in the incident beam. They are Lasermetrics, Model LM-1, transverse field, Pockels cells. MOD3 and MOD4 in the emerging beam are longitudinal field, thin plate, Pockels cells of our own construction.[38] The crystals in all four modulators are potassium dideuterium phosphate (KD*P) with a deuteration level greater than 99%.

For MOD1 and MOD2 approximately 750 volts is required to achieve the retardation at 633 nm. specified by Eqs. 19 and 20. For these modulators the light must be collimated and parallel to the crystal axis to within a couple milliradians since off-axis light experiences a retardation independent of the applied voltage. For the laser sources, neither this nor the relatively small clear aperture (~2.5 mm) is a problem.

MOD3 and MOD4 generally operate on diffuse, scattered light. Therefore, both a larger clear aperture and a larger useable angular field are required. Both of these modulators employ a single Z-cut crystal plate 12 mm square and 3 to 5 mm thick. Chromium backed gold grids are vacuum evaporated onto both faces. A uniform

electric field, parallel to the optic axis, is produced when a potential difference is applied between the grids. Approximately 3000 volts, independent of crystal thickness, is necessary to obtain the required retardation (Eq. 20).[39] Since off axis light rays undergo retardation proportional to crystal thickness, the useable angular field is limited by crystal thickness. However, the crystal must be thick enough to prevent breakdown due to the high voltage. This is particularly a problem with A.C. voltages.[40] Our experience has shown that 3 mm and 5 mm thicknesses for MOD3 (ν_3=1.0 kHz) and MOD4 (10.0 kHz), respectively, are good compromises.

The electro-optic coefficient and the residual retardance of KD*P are strongly dependent on temperature. Therefore, to obtain long term stability, the housings of all four modulators are held at 15°C with chilled water from a constant temperature (±0.1°C) circulator. The choice of 15°C is a compromise between avoidance of condensation and reduction of the required potential difference across the crystal.

The modulators are driven by a power amplifier through a step-up transformer. For MOD1,2, and 3, iron core, audio transformers give step up ratios of 35, 80, and 275, respectively. An air core transformer giving a step up ratio of 270 is used for MOD4.

B. Detection Electronics

A schematic of the detection system is shown in Fig. 3. The

photodetector is an RCA 8645 photomultiplier tube. A servo loop controls the high voltage to the photomultiplier so as to maintain the DC component of the anode current at a constant value.[31] Since the DC component is proportional only to f_{11}, the effect is to divide all the amplitudes in the Fourier spectrum of the signal by f_{11}.

The AC signal passes through an AC amplifier and then to a high Q (~200) bandpass amplifier at the input of each of the fifteen phase sensitive detectors (PSD). The bandpass amplifier is tuned to the frequency of the corresponding matrix element f_{ij} given in Fig 2.

Reference frequencies for the PSD's are generated based on the fact that the product of two sinusoidal voltages results in sinusoidal voltages at the sum and difference frequencies. Analog multipliers are used to form the products. Bandpass filters isolate either the sum or the difference frequency and the resulting sinusoidal signal is amplified and clipped to produce a square wave. Fig. 4 shows a flow chart for the generation of the fifteen reference frequencies. The circuit for generation of a typical reference frequency is shown in Fig. 5.

The phase sensitive detectors (PSD) are based on analog multiplication of the signal from the photomultiplier with the appropriate square wave reference frequency. The Fourier component of the signal with the same frequency as the reference fre-

quency produces a DC voltage component in the product. This DC voltage is proportional to the matrix element corresponding to the reference frequency. The outputs of all fifteen PSD's (and hence fifteen matrix elements) are available simultaneously. The circuit for a typical PSD is shown in Fig. 6.

Only f_{11} remains to be determined. This can be done either directly in an independent measurement, or simultaneously by observing the high voltage to the photomultiplier tube. In the latter case, the servo loop adjusts the high voltage so as to keep the DC component of the signal (and hence f_{11}^{*}) constant. We empirically measure this functional dependence and then use it to determine f_{11} from high voltage measurements. The high voltage and the signals from the fifteen PSD's are recorded directly on an analog recorder or digitized and stored by computer for further analysis.

V. ALIGNMENT AND CALIBRATION

Proper alignment and calibration of the instrument involves the following adjustments:

a) As the detector sweeps through scattering angles it defines a plane. The incident laser beam must be adjusted so that it lies in this plane.

b) The reference plane for defining the Stokes vectors must be defined. In this instrument we have chosen it to coincide with the scattering plane. Thus the transmission axes of POL1 and POL2 must be positioned to be in the scattering plane.

c) The yaw and pitch of the modulators must be adjusted so that the light beam is parallel to their optic axes.

d) The azimuth angles γ_i of the modulators must be set to the values given in Fig. 1.

e) The retardation amplitudes δ_{0i} must be made to satisfy Eq. (19).

f) The gains of the DC amplifiers in the PSD's must be set so that the outputs correspond to matrix elements varying between ±1.0.

The complete alignment and calibration procedure is described by Thompson.[38] The adjustments a) and b) above are straightforward. We will briefly describe those involved in c) through e).

Misalignment of the light beam and modulator axes appears as a constant retardation. In a first order analysis we represent the

retardance of each modulator by

$$\delta_i = \delta_{ci} + \delta_{oi} \cos \omega_i t \ , \tag{23}$$

where δ_{ci} is the constant retardation. The completely general Mueller matrix representing a retarder with retardance δ and with fast axis at an arbitrary angle γ with respect to the reference plane is given by Simmons and Guttmann,[3]

$$M_{ret} = \begin{vmatrix} 1 & 0 & 0 & 0 \\ 0 & \cos^2 2\gamma + \sin^2 2\gamma \cos\delta & \tfrac{1}{2} \sin 4\gamma (1-\cos\delta) & \sin 2\gamma \sin\delta \\ 0 & \tfrac{1}{2} \sin 4\gamma (1-\cos\delta) & \sin^2 2\gamma + \cos^2 2\gamma \cos\delta & -\cos 2\gamma \sin\delta \\ 0 & -\sin 2\gamma \sin\delta & \cos 2\gamma \sin\delta & \cos\delta \end{vmatrix} \tag{24}$$

We use these matrices in Eq. (12) to derive the general form of the detected intensity. In addition to our original result which assumed perfect alignment, the Fourier expansion of this result contains some terms at the four primary frequencies and some terms which mix matrix elements. Specifically the latter terms are proportional to one matrix element but are at a frequency corresponding to a different matrix element. These additional terms are listed in Fig. 7 to first order in the small quantities:

$$\begin{aligned} &\sin(\delta_{ci}) \ , \ i = 1, 2, 3, 4 \ ; \\ &J_0(\delta_{oi}) \ , \ i = 1, 2, 3, 4 \ ; \\ &\cos(2\gamma_i) \ , \ i = 1, 4 \ ; \\ &\sin(2\gamma_i) \ , \ i = 2, 3 \ . \end{aligned} \tag{25}$$

Also, in Fig. 7 we have used the following relations which are correct to first order:

$$\begin{aligned} &\cos(\delta_{ci})=1, \quad i = 1, 2, 3, 4, \ ; \\ &\sin(2\gamma_i)=1, \quad i = 1, 4 \ ; \\ &\cos(2\gamma_i)=1, \quad i = 2, 3 \ . \end{aligned} \tag{26}$$

Any factor multiplying an f_{ij} in Fig. 7 is to be made zero by the proper alignment of the system. The procedure is to substitute an optical device with known Mueller matrix for F and to set the detector arm at $\theta=0$; see Fig. 1. Specifically, we select an optical device for which the matrix element being measured is identically zero and the mixing matrix element is large. The appropriate adjustment is then made to minimize the mixing term. The optical devices used are linear polarizers, wave plates, combinations of the two, and empty space. The latter is the unity matrix.

In order to calibrate the full scale amplitudes, optical devices are inserted into the sample space. The gains of the amplifiers in the PSD's are adjusted to give 2.5 volts full scale if the corresponding matrix element is unity. Empty space is used to calibrate f'_{22}, f'_{33}, and f'_{44}. A rotating crystal polarizer is used for f'_{12}, f'_{21}, f'_{13}, f'_{31}, f'_{23}, and f'_{32}. A rotating quarter-wave plate is used for f'_{24}, f'_{42}, f'_{34}, and f'_{43}; the quarter wave plate retardance is independently checked by measuring the previously cali-

brated f'_{44}. Finally, f'_{14} and f'_{41} are calibrated by using the quarter wave plate and a rotating polarizer together.

After alignment and calibration, the accuracy of the instrument is always better than 5%. By waiting for complete temperature stabilization and by carefully iterating the alignment-calibration procedure several times, the instrument provides 1% measurements. These accuracy determinations are made by measuring the matrices of known optical devices and represent maximum observed errors.

VI. EXPERIMENTAL RESULTS

Mueller matrices for a number of optical devices and scattering systems have been measured. Some were for purposes of evaluating the operation of the instrument while others[41-42] were of independent interest. In Fig. 8 we show the matrix for a Glan-Taylor polarizer. For these measurements the detector is set at 0^{o}, and the polarizer is placed in the sample space and rotated at 1.0 rpm. The results are presented in Fig. 8 in matrix form with each graph at the position of the corresponding matrix element. The graphs give the value of the matrix element as a function of the angle ψ between the transmission axis and the reference plane. The normalized matrix for an ideal linear polarizer is

$$F_{pol} = \begin{vmatrix} 1 & \cos 2\psi & \sin 2\psi & 0 \\ \cos 2\psi & \cos^2 2\psi & \tfrac{1}{2}\sin 4\psi & 0 \\ \sin 2\psi & \tfrac{1}{2}\sin 4\psi & \sin^2 2\psi & 0 \\ 0 & 0 & 0 & 0 \end{vmatrix} . \qquad (27)$$

Six of these matrix elements were, in fact, used to calibrate the instrument. For the others there is excellent agreement between Fig. 8 and Eq. (27).

In Fig. 9, we show the results for a mounted Mica retarder at a wavelength of 442 nm. This particular device had nominally quarter wave retardance at 663 nm. Data are obtained in the same fashion as with the linear polarizer. The abscissa is the angle γ between

the retarder fast axis and the reference plane. The matrix for an ideal linear retarder is given by Eq. (24). Comparing the data with Eq. (24) we find the retardance is $120^{0}\pm2^{0}$ at 442 nm.

Fig. 10 shows the Mueller matrix for scattering by a suspension of polystyrene microspheres in water. The mean diameter of the spheres is 0.091μ, and the standard deviation is 0.006μ. For these data the abscissa is the scattering angle θ. The laser wavelength is 633 nm. For this particle size the scattering is very Rayleigh like. Mie[11] calculations of the matrix elements for the specified particle distribution are generally indistinguishable from these data and are not shown.

Finally Fig. 11 shows the matrix for a single polystyrene sphere. The sphere is suspended in air in an inhomogeneous electric field.[42] The laser wavelength is 442 nm. Mie calculations, using 1.110μ for the sphere diameter and 1.6144 for the index of refraction, are also shown. The agreement is good.

VII. SUMMARY

An instrument which provides for simultaneous measurement of all sixteen elements of Mueller matrices has been described. Important features are:

(1) A fixed linear polarizer precedes the photodetector. Thus the polarization of the observed light never changes and polarization sensitivities in the detector cannot introduce errors.

(2) Relatively rapid measurements can be made so that samples undergoing changes can be studied (e.g. biological systems, chemical reactions, or settling phenomena).

(3) Accuracies of 3% are easily achieved and have been demonstrated by measuring the matrices for known optical devices.

(4) The same hardware can be used at different wavelengths by simply adjusting the voltages applied to the modulators so as to maintain the required retardation amplitudes δ_{0i}.

(5) Instrument calibration can be completely traced to empty space and to a linear polarizer.

The work presented here has been supported by the Office of Naval Research, Code 480, under Grant No. N00014-75-C-0537.

REFERENCES

1. F. Perrin, J. Chem Phys 10, 414 (1942).
2. H. C. Van de Hulst, "Light Scattering by Small Particles" (John Wiley and Sons, New York, 1957).
3. J. W. Simmons and M. J. Guttmann, "States, Waves and Photons: A Modern Introduction to Light" (Addison-Wesley, Reading, Massachusetts, 1970).
4. G. W. Kattawar, G. N. Plass and J. A. Guinn, Jr., J. Phys. Oceanogr. 3, 353 (1973).
5. S. J. Hitzfelder, G. N. Plass, and G. W. Kattawar, Appl. Opt. 15, 2489 (1976).
6. G. W. Kattawar and G. N. Plass, Appl. Opt. 15, 3166 (1976).
7. G. W. Kattawar and G. N. Plass, and C. N. Adams, Ap. J. 170, 371 (1971).
8. YE. A. Kadyshevich, YU. S. Lyubovtseva, and I. N. Plakhina, Atmos. and Ocean. Phys. 7, 367 (1971).
9. YE. A. Kadyshevich and YU. S. Lyubovtseva, Atmos. and Ocean. Phys. 9, 659 (1973).
10. YE. A. Kadyshevich, YU. S. Lyubovtseva, and G. V. Rozenberg, Atmos. and Ocean. Phys. 12, 106 (1976).
11. G. Mie, Ann. Phys. 25; 377 (1908).
12. Lord Rayleigh, Phil. Mag. 36, 365 (1918).
13. J. R. Wait, Can. J. Phys. 33, 189 (1955).
14. S. Asano and G. Yamamoto, Appl. Opt. 14, 29 (1975).
15. E. M. Purcell and C. R. Pennypacker, Ap. J. 186, 705 (1973).

16. G. W. Kattawar and T. J. Humphreys, submitted to Appl. Opt. (1979).

17. C. Yeh, in "Proceedings of the International Workshop on Light Scattering by Irregularly Shaped Particles", ed. D. Schuerman, Plenum Pub. Corp., N.Y., 1980.

18. B. S. Pritchard and W. G. Elliott, J. Opt. Soc. Am. 50, 191 (1960).

19. G. V. Rozenberg, Adv. in Phys. Sciences 11, 353 (1968).

20. G. I. Gorchakov and G. V. Rozenberg, Atmos. and Ocean. Phys. 3, (1967).

21. A. C. Holland and G. Gagne, Appl. Opt. 5, 1113 (1970).

22. G. F. Beardsley, Jr., J. Opt. Soc. Am. 58, 52 (1968). Complete references to this work can be found in ref. 10.

23. J. C. Kemp, J. Opt. Soc. Am. 59, 950 (1969).

24. L. F. Mollenauer, D. Downie, H. Engstrom, and W. B. Grant, Appl. Opt. 8, 661 (1969).

25. J. C. Kemp, R. D. Wolstencroft, and J. B. Swedlund, Ap. J. 177, 177 (1972).

26. J. Tinbergen, Astr. and Ap. 23, 25 (1973).

27. G. R. Boyer, B. F. Lamouroux, and B. S. Prade, Appl. Opt. 18, 1217 (1979).

28. D. E. Aspnes and A. A. Studna, Appl. Opt. 14. 220 (1975).

29. C. Cortese, F. Aramu, and V. Maxia, Opt. Commun. 2, 296 (1975).

30. P. S. Hauge, Proc. SPIE 88, 3 (1976).

31. A. J. Hunt and D. R. Huffman, Rev. Sci. Instrum. 44, 1753 (1973).

32. R. C. Thompson and E. S. Fry, J. Opt. Soc. Am. 64, 1399 (1974).

33. R. J. Perry, A. J. Hunt, and D. R. Huffman, Appl. Opt. 17, 2700 (1978).

34. W. S. Bickel, J. F. Davidson, D. R. Huffman, and R. Kilkson, Proc. Nat. Acad. Sci. USA, 73 486 (1976).

35. R. M. A. Azzam, Opt. Lett. 2, 148 (1978).

36. R. C. Thompson, J. Opt. Soc. Am. 66, 1134 (1976).

37. R. C. Thompson, E. S. Fry, and J. R. Bottiger, Proc. SPIE 112, 152 (1977).

38. R. C. Thompson, "An Electro-optic Light Scattering Photometric Polarimeter" Ph.D thesis, Texas A&M University (1978).

39. R. Goldstein, "Pockel's Cell Primer", Laser Focus, p. 21 (Feb. 1968).

40. B. H. Billings, J. Opt. Soc. Am. 39, 802 (1949).

41. R. C. Thompson, J. R. Bottiger and E. S. Fry, Proc. SPIE 160, 43 (1978).

42. J. R. Bottiger, E. S. Fry, and R. C. Thompson, in "Proceedings of the International Workshop on Light Scattering by Irregularly Shaped Particles", ed. D. Schuerman, Plenum Pub. Corp. N.Y., 1980.

Table I

Values of $J_n(\delta_0)$; $\delta_0 = 2.404$ radians

$J_0(\delta_0) = 0.0$	$J_5(\delta_0) = 0.016$
$J_1(\delta_0) = 0.520$	$J_6(\delta_0) = 0.0036$
$J_2(\delta_0) = 0.431$	$J_7(\delta_0) = 0.00059$
$J_3(\delta_0) = 0.198$	$J_8(\delta_0) = 0.00009$
$J_4(\delta_0) = 0.064$	$J_9(\delta_0) = 0.00001$

FIGURE CAPTIONS

Fig. 1. Schematic of the instrument. The angle θ is the scattering angle. The orientations of the transmission axes and fast axes of the polarizers and retarders, respectively, are given by γ.

Fig. 2. The linear combinations of primary frequencies at which each matrix element appears in first order in the output intensity is shown. The numerical value of the frequency at which we observe each matrix element is also given.

Fig. 3. Schematic of the electronics.

Fig. 4. Flow chart for generation of the various reference frequencies. Analog multipliers are used to produce the sum and difference frequencies.

Fig. 5. Circuit for generating a reference frequency. Standard operational amplifiers and analog multipliers are used. Capacitor, resistor, and inductor values depend on the particular reference frequency.

Fig. 6. Circuit for phase sensitive detector (PSD). Standard operational amplifiers and analog multipliers are used.

Fig. 7. First order terms which arise due to misalignment of the optical system. They are presented in the positions corresponding to the reference frequencies at which they appear.

Fig. 8. Measured matrix of a linear polarizer. The abscissa is the angle between the transmission axis and the reference plane.

Fig. 9. Measured matrix of a linear retarder at 442 nm. This was nominally a quarter wave retarder at 633 nm.

Fig. 10. Measured matrix of an aqueous suspension of 91.0 nm. diameter polystyrene spheres. The wavelength is 633 nm. This is a very Rayleigh-like system and the data are nearly indistinguishable from Mie calculations.

Fig. 11. Measured matrix for a single polystyrene sphere suspended in air in an inhomogeneous electric field. The dotted curves are Mie calculations using a diameter of 1.110 micron and an index of refraction of 1.6144.

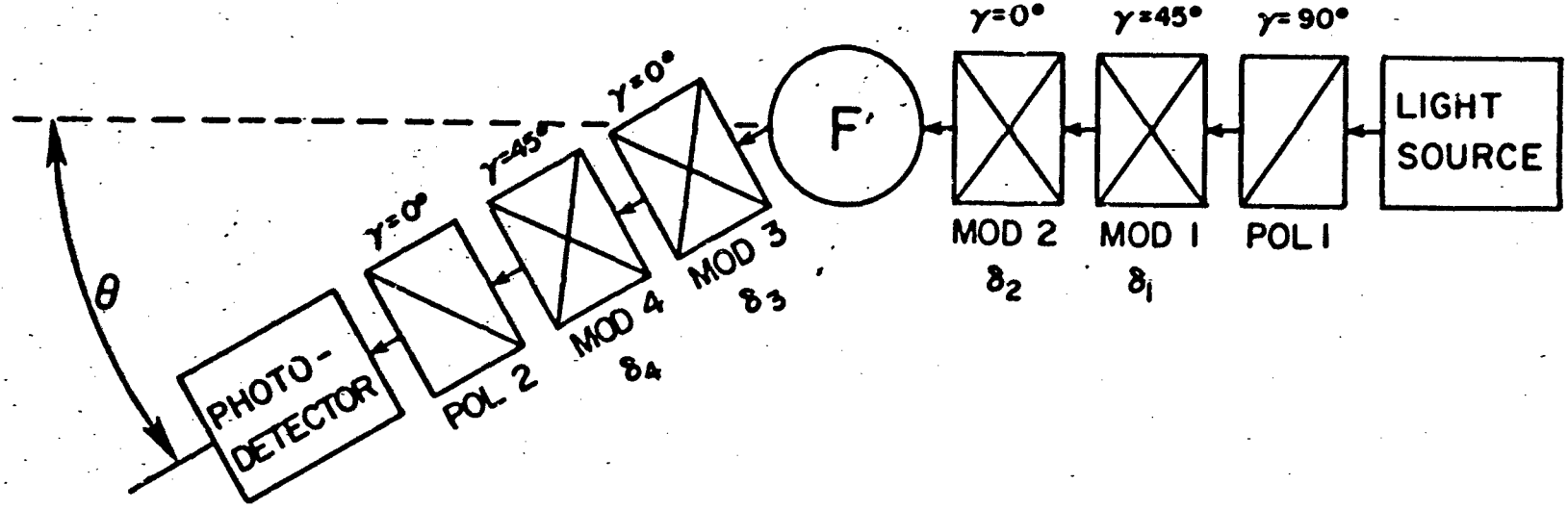

Fig. 1. Schematic of the instrument. The angle θ is the scattering angle. The orientations of the transmission axes and fast axes of the polarizers and retarders, respectively, are given by γ.

f_{11} D.C.	f_{12} $2\omega_1$ 82.0	f_{13} $\omega_1 \pm \omega_2$ 40.7	f_{14} $\omega_1 \pm 2\omega_2$ 41.6
f_{21} $2\omega_4$ 20.0	f_{22} $2\omega_1 \pm 2\omega_4$ 62.0	f_{23} $\omega_1 \pm \omega_2 \pm 2\omega_4$ 60.7	f_{24} $\omega_1 \pm 2\omega_2 \pm 2\omega_4$ 21.6
f_{31} $\omega_3 \pm \omega_4$ 9.0	f_{32} $2\omega_1 \pm \omega_3 \pm \omega_4$ 91.0	f_{33} $\omega_1 \pm \omega_2 \pm \omega_3 \pm \omega_4$ 49.7	f_{34} $\omega_1 \pm 2\omega_2 \pm \omega_3 \pm \omega_4$ 32.6
f_{41} $2\omega_3 \pm \omega_4$ 12.0	f_{42} $2\omega_1 \pm 2\omega_3 \pm \omega_4$ 70.0	f_{43} $\omega_1 \pm \omega_2 \pm 2\omega_3 \pm \omega_4$ 28.7	f_{44} $\omega_1 \pm 2\omega_2 \pm 2\omega_3 \pm \omega_4$ 53.6

Fig. 2. The linear combinations of primary frequencies at which each matrix element appears in first order in the output intensity is shown. The numerical value of the frequency at which we observe each matrix element is also given.

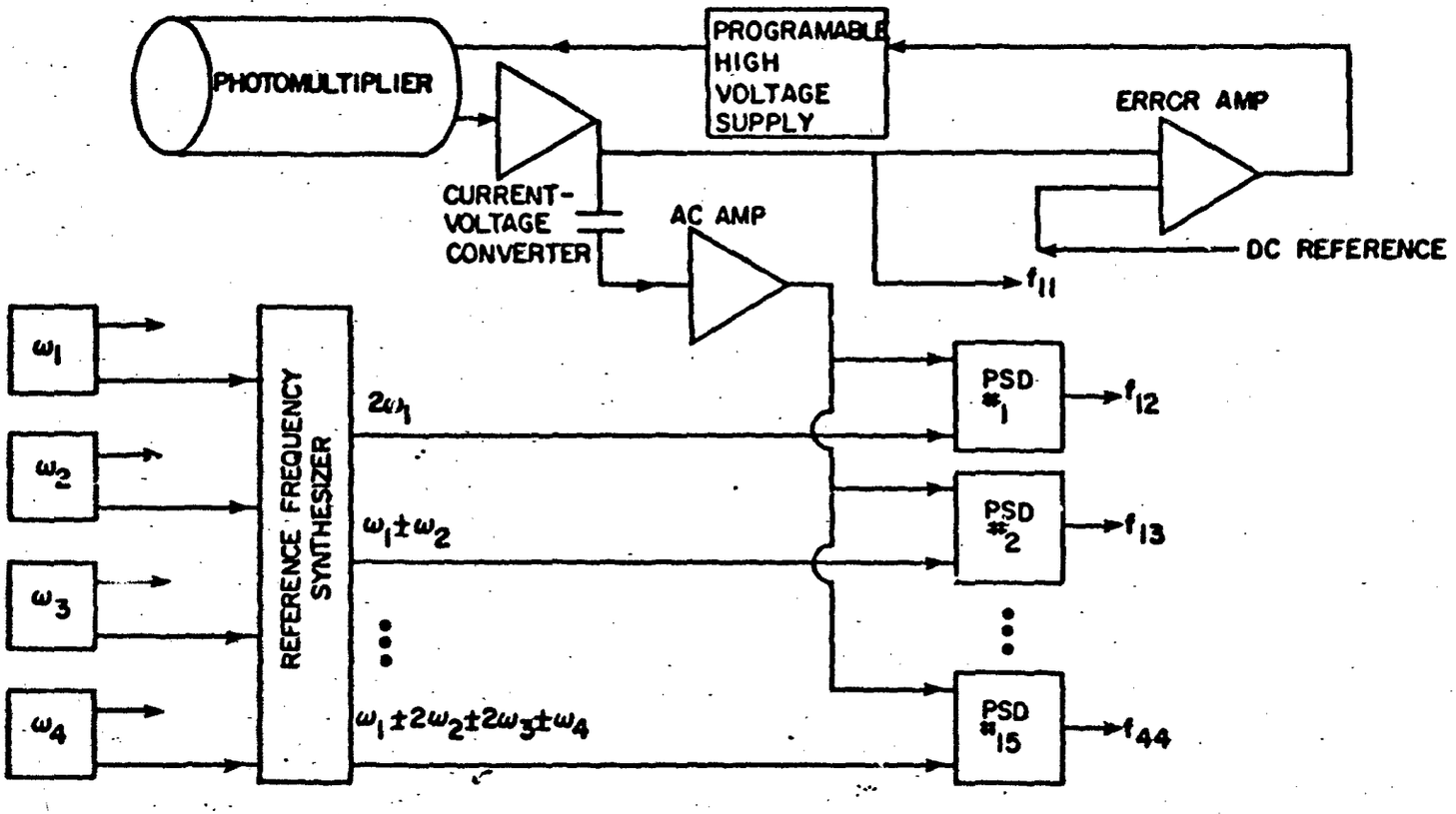

Fig. 3. Schematic of the electronics.

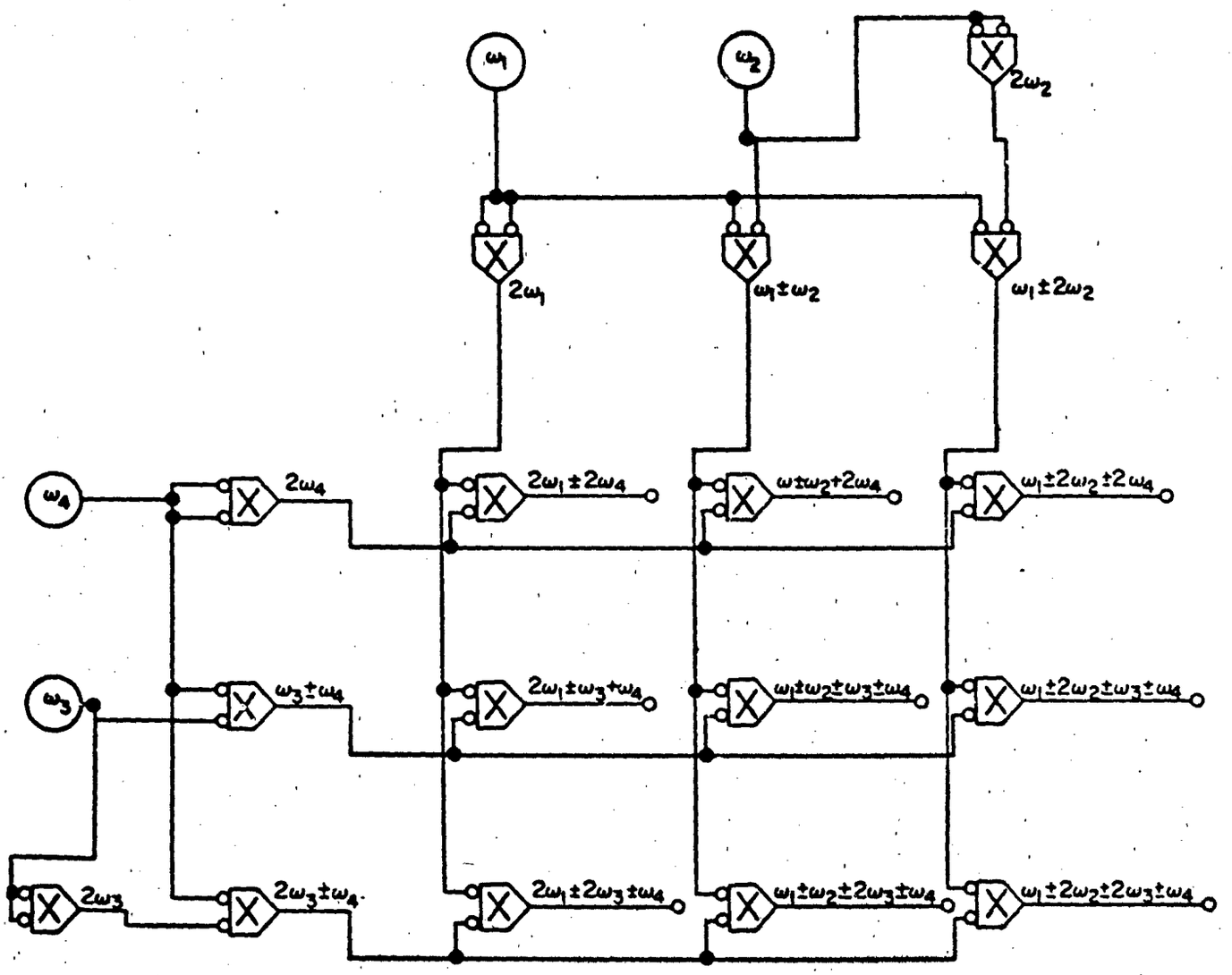

Fig. 4. Flow chart for generation of the various reference frequencies. Analog multipliers are used to produce the sum and difference frequencies.

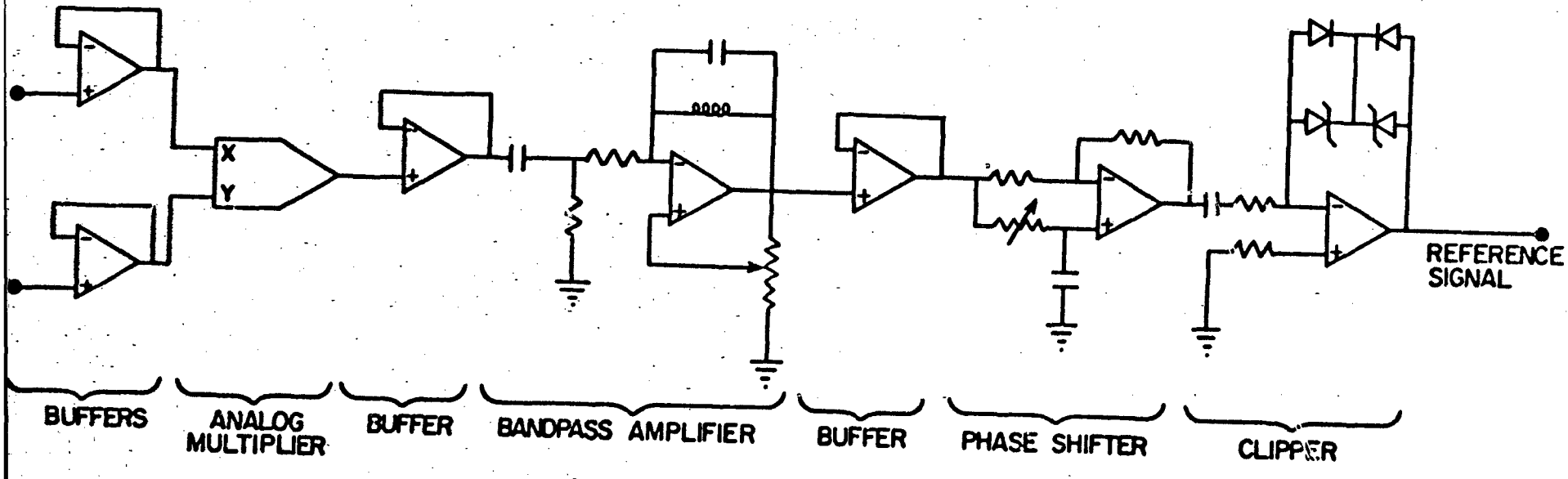

Fig. 5. Circuit for generating a reference frequency. Standard operational amplifiers and analog multipliers are used. Capacitor, resistor, and inductor values depend on the particular reference frequency.

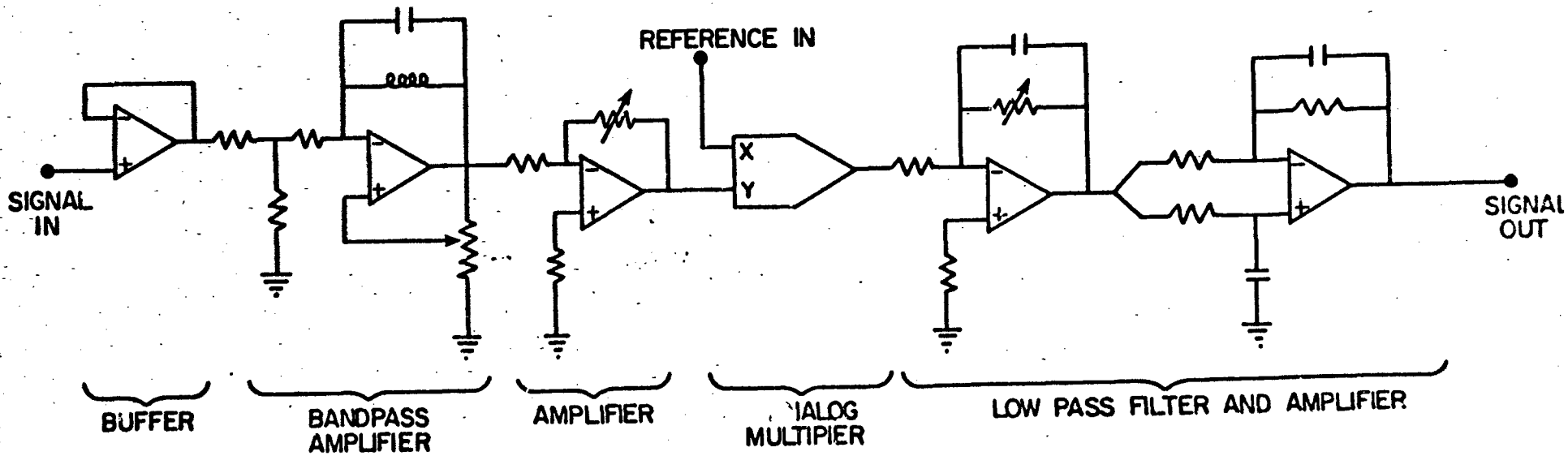

Fig. 6. Circuit for phase sensitive detector (PSD). Standard operational amplifiers and analog multipliers are used.

f_{11} $f_{12} J_0(\delta_{01})$ $+f_{21} J_0(\delta_{04})$	f_{12} $f_{13} \sin(2\gamma_2)$ $+f_{22} J_0(\delta_{04})$	f_{13} $f_{12} \sin(2\gamma_2)$ $+f_{14} \sin(\delta_{c2})$ $+f_{23} J_0(\delta_{04})$	f_{14} $+f_{13} \sin(\delta_{c2})$ $+f_{24} J_0(\delta_{04})$
f_{21} $f_{22} J_0(\delta_{01})$ $+f_{31} \sin(2\gamma_3)$	f_{22} $f_{23} \sin(2\gamma_2)$ $+f_{32} \sin(2\gamma_3)$	f_{23} $f_{22} \sin(2\gamma_2)$ $+f_{24} \sin(\delta_{c2})$ $+f_{33} \sin(2\gamma_3)$	f_{24} $f_{23} \sin(\delta_{c2})$ $+f_{34} \sin(2\gamma_3)$
f_{31} $f_{21} \sin(2\gamma_3)$ $+f_{32} J_0(\delta_{01})$ $+f_{41} \sin(\delta_{c3})$	f_{32} $f_{22} \sin(2\gamma_3)$ $+f_{33} \sin(2\gamma_2)$ $+f_{42} \sin(\delta_{c3})$	f_{33} $f_{23} \sin(2\gamma_3)$ $+f_{32} \sin(2\gamma_2)$ $+f_{34} \sin(\delta_{c2})$ $+f_{43} \sin(\delta_{c3})$	f_{34} $f_{24} \sin(2\gamma_3)$ $+f_{33} \sin(\delta_{c2})$ $+f_{44} \sin(\delta_{c3})$
f_{41} $f_{31} \sin(\delta_{c3})$ $+f_{42} J_0(\delta_{01})$	f_{42} $f_{32} \sin(\delta_{c3})$ $+f_{43} \sin(2\gamma_2)$	f_{43} $f_{33} \sin(\delta_{c3})$ $+f_{42} \sin(2\gamma_2)$ $+f_{44} \sin(\delta_{c2})$	f_{44} $f_{34} \sin(\delta_{c3})$ $+f_{43} \sin(\delta_{c2})$

ω_1: $f_{12} \sin(\delta_{c1}) + f_{14} J_0(\delta_{02})$

ω_2: $f_{14} \cos(2\gamma_1)$

ω_3: $f_{41} \cos(2\gamma_4)$

ω_4: $f_{21} \sin(\delta_{c4}) + f_{41} J_0(\delta_{03})$

Fig. 7. First order terms which arise due to misalignment of the optical system. They are presented in the positions corresponding to the reference frequencies at which they appear.

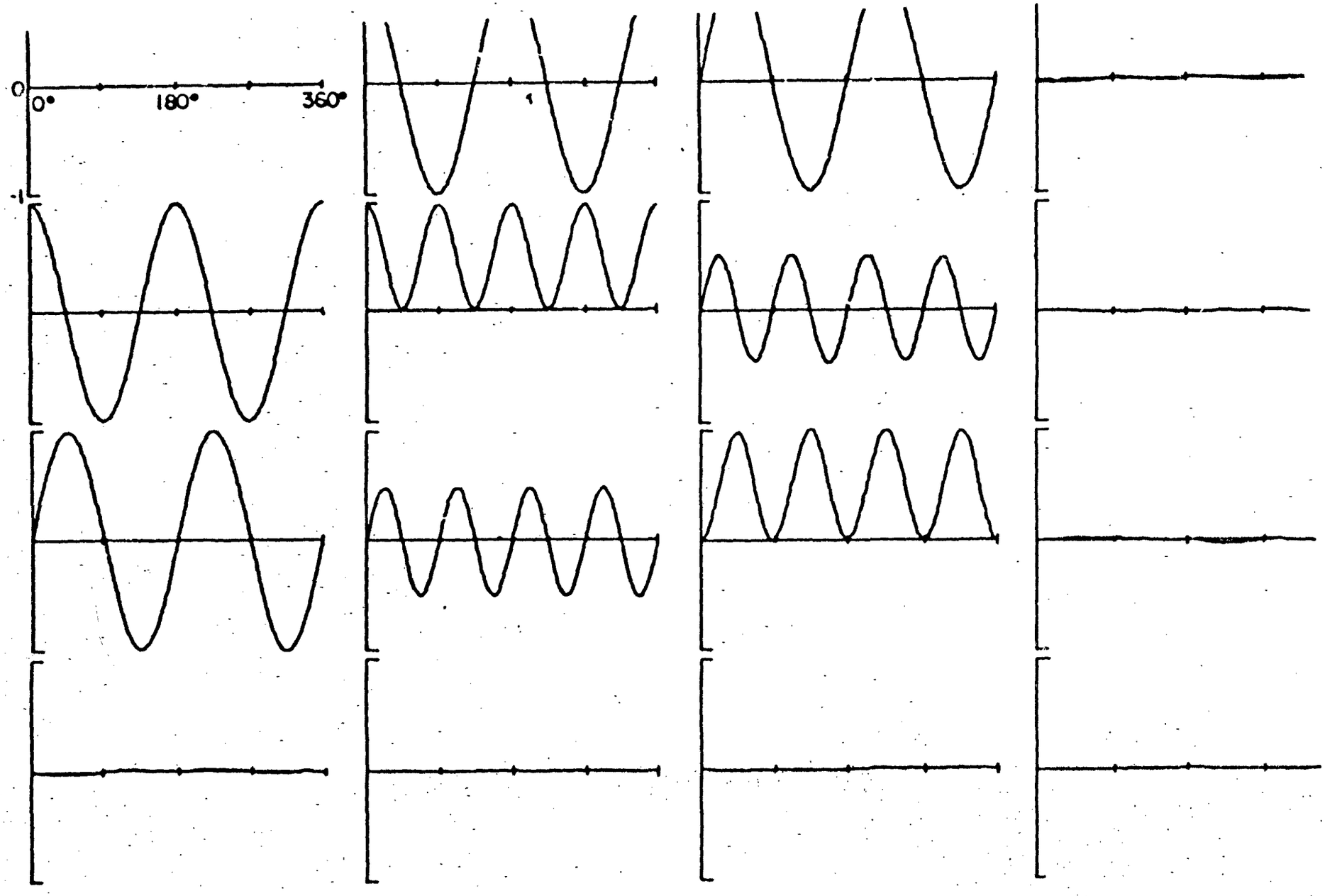

Fig. 8. Measured matrix of a linear polarizer. The abscissa is the angle between the transmission axis and the reference plane.

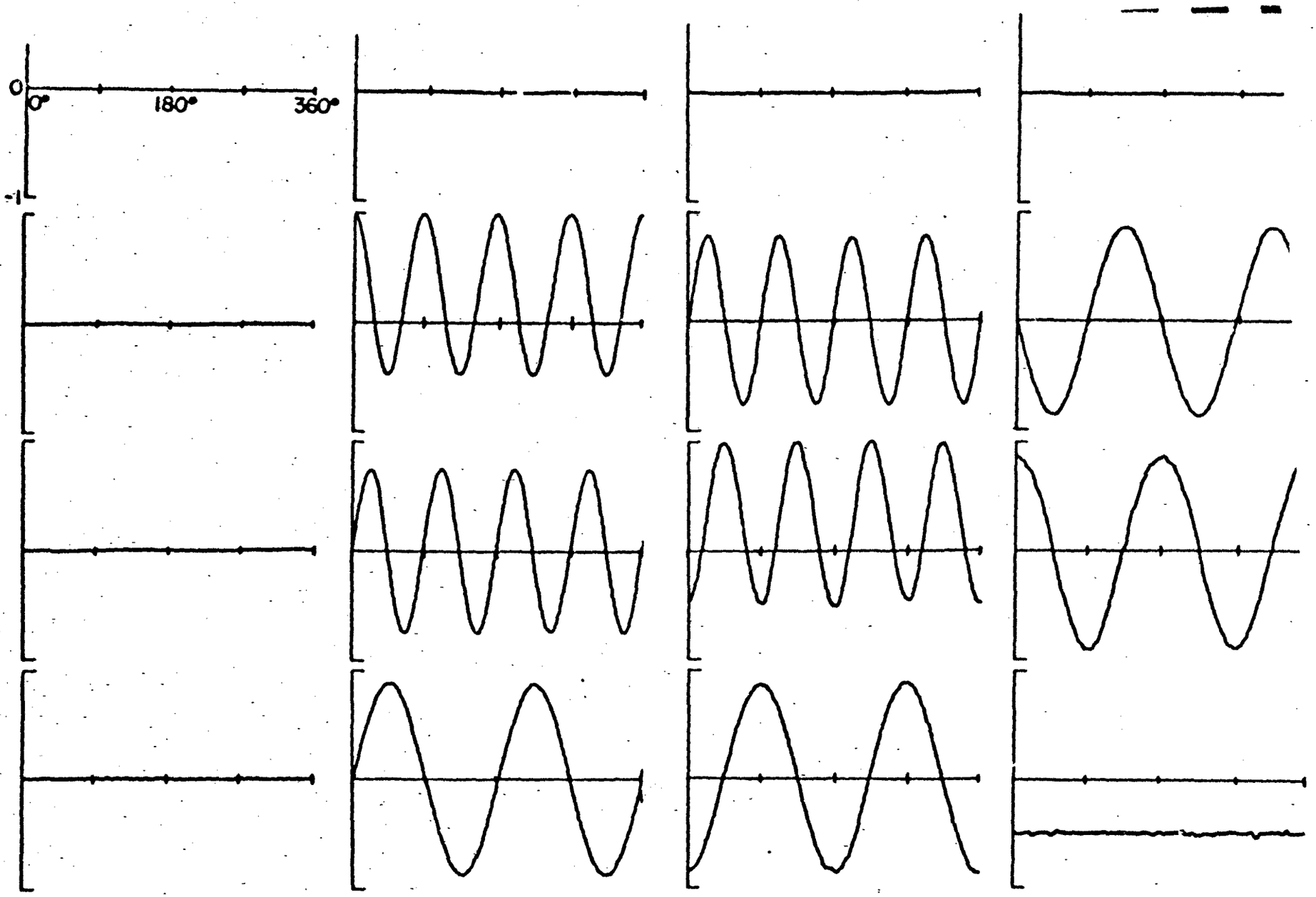

Fig. 9. Measured matrix of a linear retarder at 442 nm. This was nominally a quarter wave retarder at 633 nm.

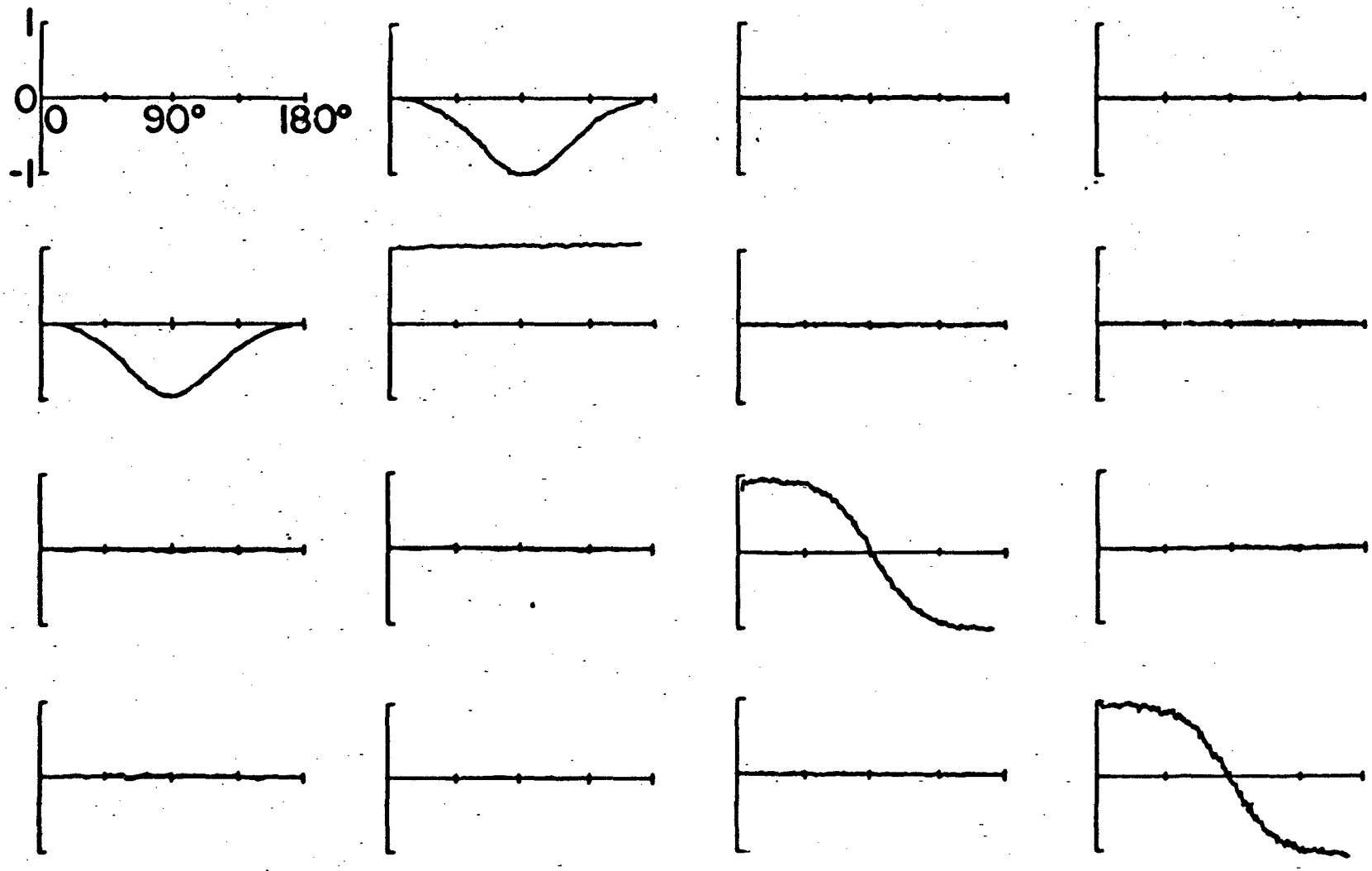

Fig. 10. Measured matrix of an aqueous suspension of 91.0 nm. diameter polystyrene spheres. The wavelength is 633 nm. This is a very Rayleigh-like system and the data are nearly indistinguishable from Mie calculations.

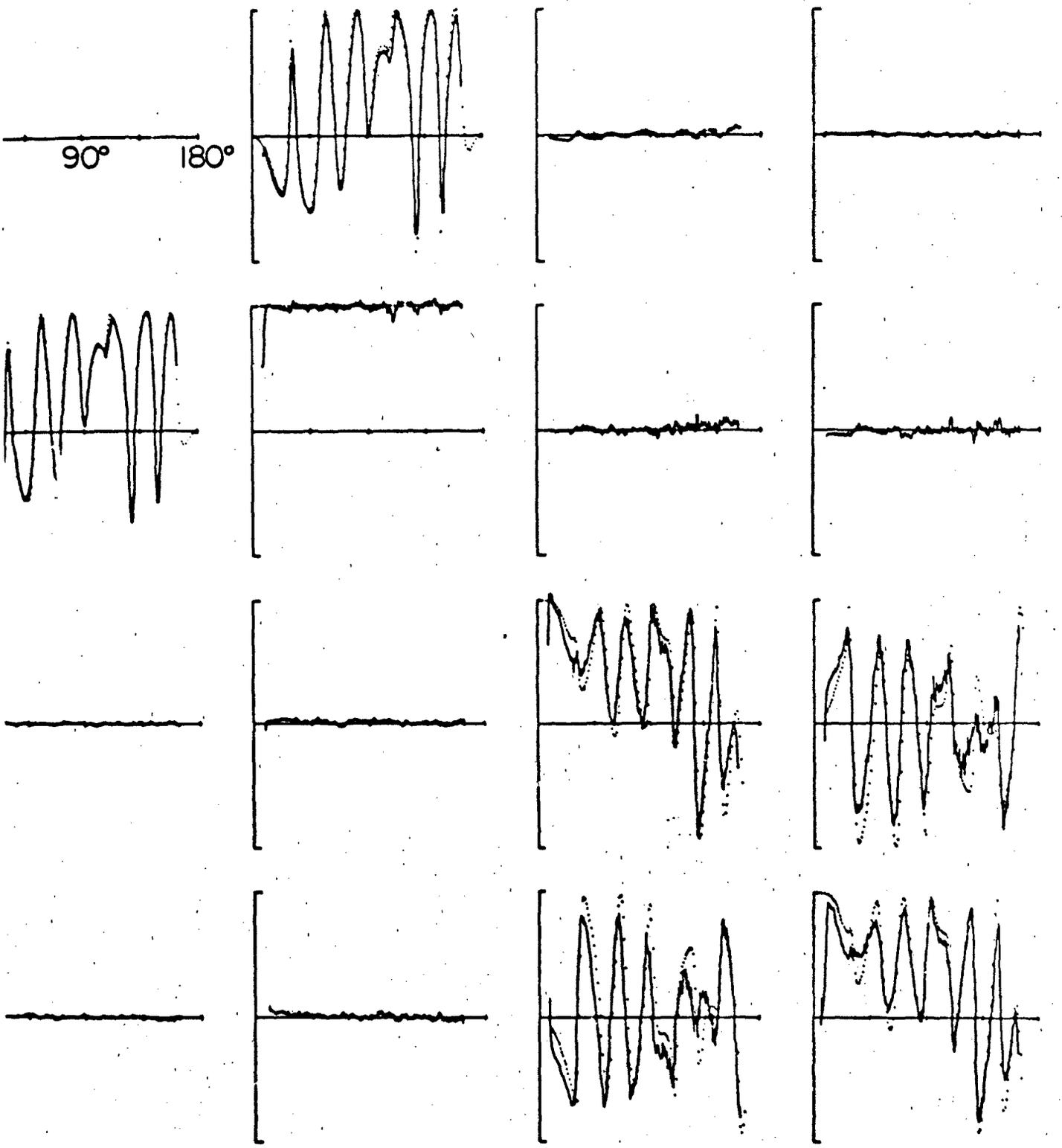

Fig. 11. Measured matrix for a single polystyrene sphere suspended in air in an inhomogeneous electric field. The dotted curves are Mie calculations using a diameter of 1.110 micron and an index of refraction of 1.6144.